Simulating an implementation of the surface code in silicon*

Gavin Dold, Sofia Qvarfort, and Simon Schaal
Centre for Doctoral Training in Delivering Quantum Technologies
Department of Physics and Astronomy, University College London
(Dated: June 7, 2016)

We simulate a simple system consisting of one probe qubit and four data qubits as proposed in [**?**] and implement errors such as dephasing, dopant displacement, and path jitter to the full stabiliser measurement cycle.

CONTENTS

I. INTRODUCTION

It is generally agreed upon that large-scale, universal quantum computing will require some form of error correction.

There has been a recent proposal to make use of dopants in silicon to act as qubits [**?**] to implement a version of the surface code.

We have simulated a probe qubit interacting with four data qubits. The probe qubit is performing a circular orbit 40 nm above the data qubits, and in this document we will document the effect of various errors. These errors include dephasing, dopan placement uncertainties and a path jitter.

A. The surface code

B. A physical implementation

In a paper in 2015, it awas proposed by G'Orman *et al.*

	T_1^e	T_2^{e*}	T_2^e	$T_{2,decoupl}^e$	T_1^N	T_2^{N*}	T_2^N
P (nat. Si, SET) [**?**]	0.7 s	55 ns	206 μs	410 μs			
P (puri. Si, SET) [**?**]		160 μs	1 ms	560 ms		500 μs	1.75
Bi (puri. Si, CT) [**?**]	9 s		2.7 s				
NV (puri. C, RT) [**?** **?**]			1.8 ms	3.3 ms			
NV (puri. C, 77 K) [**?**]				0.6 s			
SiC (20 K) [**?**]		1.1 μs	1.2 ms				
SiC (RT) [**?**]	185 μs	214 ns	40 μs				

TABLE I: [**?** **?**]: high field >1T low temp mK. Even good coherenc ebeing close to suurface.

Let us first take a closer look at the scheme proposed in [**?**]. The data qubits are dopants placed in silicon placed in a square pattern using the best dopant placement techniques available, which currently stand at [insert some error value and cite it]. To perform the stabiliser measurements, a probe qubit of a different dopant species is placed on a mobile slab above the data qubits. Each probe qubit performs a stabiliser measurement on four data qubits, a procedure which is performed by physically moving the overhead slab with the probe qubits.

Some differences in physical parameters are required.

II. SPIN SPECIES

Donors deep in bulk show longer coherence times $T_2^e = 2\,\mathrm{s}$ [**?**] not applicable for us.

III. THE SIMULATION

In this section, we will describe how we go about simulating the interaction between the probe qubit and the data qubit. The interaction is governed by the following Hamiltonian:

$$H = \mu_B B(g_1\sigma_1^Z + g_2\sigma_2^Z) + \frac{J}{r^3}(\sigma_\mathbf{1}\cdot\sigma_\mathbf{2} - 3(\hat{\mathbf{r}}\cdot\sigma_\mathbf{1})(\hat{\mathbf{r}}\cdot\sigma_\mathbf{2})) \quad (1)$$

The effect of this Hamiltonian is to evolve the probe qubit in a particular direction depending on the state of the data qubit. By initialising the probe qubit in the $|+\rangle$ state, the final parity measurement will entail finding the probe qubit in either the $|+\rangle$ state (even parity) or in the $|-\rangle$ state. This can be understood by the fact that each data qubit imparts a $\frac{\pi}{2}$ phase in

* The authors would like to thank Dan Browne and John Morton for fruitful discussions.

A. Finding the correct evolution time

The speed of the simulation is set by the total time it takes to complete one full cycle. We want the accumulated phase for an even parity measurement to reach 2π exactly. The plot in Figure **??** shows the accumulated phase as a function of evolution time.

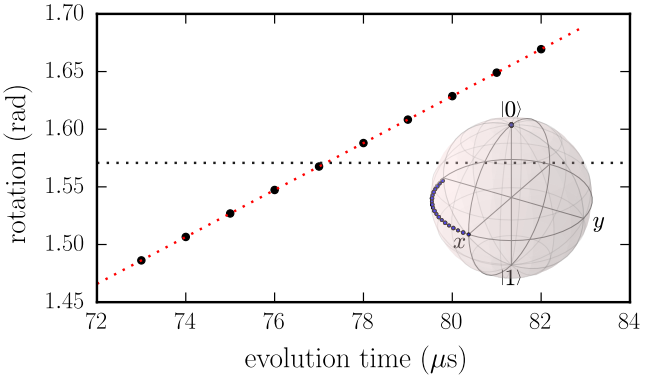

(a)

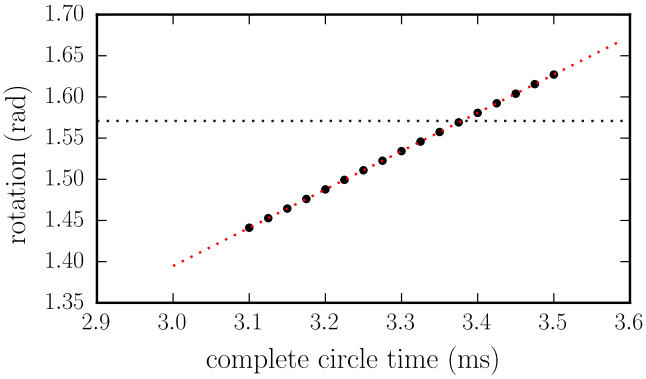

(b)

FIG. 1: Finding the correct evolution time. (a) abrupt. (b) circular

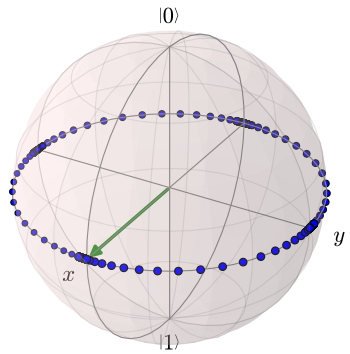

(a)

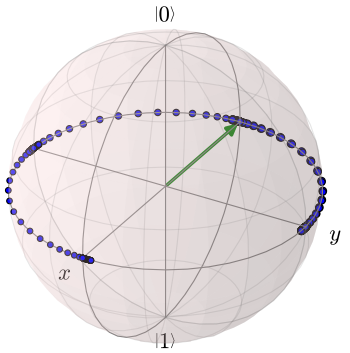

(b)

FIG. 2: Example of parity measurement for the circular motion. (a) no error in data qubits. plus state is final state. (b) error on last qubit. minus state is final state.

IV. ERRORS

In this section, we will present three types of errors that we implemented in the simulation: path jitter, dephasing and data qubit displacement. The path jitter is implemented in the calculation of the Hamiltonian for each new spatial point, whereas the dephasing is introduced through a Lindblad operator. Finally, data qubit displacement is simulated by a random offset for each of the four data qubits. In connection to qubit displacement, we will also review a technique called twirling and show how it affects our simulations. Let us begin by introducing a path jitter into the simulation.

A. Error benchmarking

There are two different ways to quantify error, and we shall here quickly review them as they will be used extensively in the following sections.

The first way to quantify error is to look at the phase ϕ accumulated by the probe qubit through the interaction with the data qubits. In [**?**], the phase jitter is defined as

$\phi + \delta$, where δ is a small deviation from $\frac{\pi}{2}$, which is the ideal phase accumulated through one quarter of the cycle. In the paper, it was found that a phase jitter of 4.4% did not have a substantial impact on the fault-tolerance threshold. We will therefore attempt to compare the phase error in our simulation with this value whenever possible. It should be noted, however, that the data we have access to usually concerns the entire run. We will therefore compare the phase error with 2π or π. We have made the assumption that the phase error stacks, such that the percentage is preserved.

B. Path Jitter

The fist error that we shall introduce is jitter present in the orbit performed by the probe qubit. The precision provided by modern MEMS control structures is about 1 nm [**?**] and is due to improve in the near future, but that does ont leave it impervious to noise. At first, we attempted to simulate random jumpts in the trajectory, but discontinuities in the path led to large derivative terms which in turn caused the simulation to fail. Instead, we superposed a sinusoidal motion onto the trajectory path. To add a random element, we varied the phase with which the run start while selecting the amplitude of the motion to represent the uncertainty in precision. The results can be found in Figure 3, where we note that an uncertainty of about 2 nm is sufficient for staying below the phase error threshold of 4.4%. Here, we are not comparing the phase jitter with the measurement probability since the probe qubit is not undergoing dephasing due to this interaction. It is sufficient to look at jitter in the y-direction instead of both the x and y direction, since the phase error is symmetric between them.

From the graph it also becomes clear that jitter in the z-direction has the greatest influence. This is due to the $\frac{1}{r^3}$ term in the Hamiltonian which favours the influence of the z-direction.

C. Dephasing

Next, we looked at the influence of dephasing on the measurement probabilities. In order to simulate dephasing, which is the gradual reduction of the Bloch vector in the x-direction, we introduced a Lindblad operator into the master equation. The operator is given by

$$L = \sqrt{\Gamma}\sigma_z, \tag{2}$$

where Γ is the dephasing parameter, which can also be written as $1/\tau$ where τ is the dephasing time. Since dephasing does not affect the phase accumulated over the four runs, we do not end up with a phase error, except when our state completely decoheres and the phase information becomes unavailable. Therefore, the only accurate measure of the error becomes the probability of

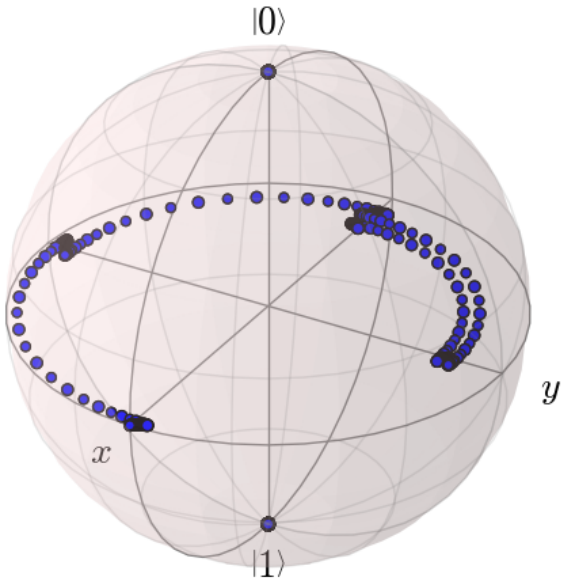

FIG. 3

correctly measuring the stabiliser in either the $|+\rangle$ (even parity) or $|-\rangle$ (odd parity). We ran simulations for both the abrupt and circular orbit using the T_2 and T_2^* values in Table **??**. The results can be found in Figure **??**, where each number refers to an entry in the table.

We see that the clock transition in Bismuth does exceptionally well, but that many spin species decohere before the run is completed. This is especially notable in the case for the circular orbit, which takes approximately 10 times longer than the abrupt orbit. It should be noted however that data for the spin species which decohere completely is for the T_2^* time measured without the aid of Hahn echoes [**?**] or dynamic decoupling [**?**]. Implementing these additional techniques would significantly improve the dephasing time for many of the proposed spin species.

As we discuss in more detail in Section **??**, the impact of dephasing could be decreased by lowering the time needed for the probe qubit to complete one orbit around the data qubits. This would require lowering the distance d between the probe qubits and the data qubits as to increase the interaction strength between them.

D. Data qubit displacement

The effect of displacement of the data qubits from the ideal was investigated. Ideally the data qubits would be in a square lattice of spins precisely $D = 400\,\text{nm}$ apart, but due to inaccuracies in dopant spin placement each qubit will have small displacements from the ideal lattice position.

This is modelled by generating a uniform random

displacement within a given pillbox xy-radius and z-height. Simulations from the original paper show radius = height = 6 nm to be a threshold for this scheme. The phase accumulated over 25 runs for this pillbox size is plotted as a histogram in fig. 5, showing a maximum phase error of $\frac{\pi}{4}$ for these runs.

The effect of displacements in the x-y plane and the z-axis are significantly different in magnitudes, due to the $\frac{1}{d^3}$ term in the Hamiltonian being most strongly affected by z displacements. This effect was investigated by artificially setting displacements in these directions.

Fig. 6a shows changes in accumulated phase due to z-displacements. The first 2 qubits are displaced 4 nm down, slowing the evolution and giving a noticeable phase error after half a cycle. However, qubit 4 is displaced 3 nm upwards, reducing d and resulting in faster evolution. The effect is a small phase error from the ideal 2π.

Fig. 6b shows the effect of displacements in the x-y plane. For this run, all data qubits were displaced 10 nm inwards with respect to the circular motion. The phase error on each individual qubit is then less than that produced by the 3 nm z-displacement of fig. 6a, showing the smaller sensitivity to displacement in the x-y plane, though the overall error after all 4 qubits is greater as in the z-direction, $+z$ and $-z$ errors cancel out somewhat, whereas xy displacement errors will always slow the evolution.

E. Twirling

V. CONCLUSIONS AND OUTLOOK

In this report, we have presented the results obtained from simulating the interaction between one probe qubit and four data qubits as in the proposed scheme in [**?**].

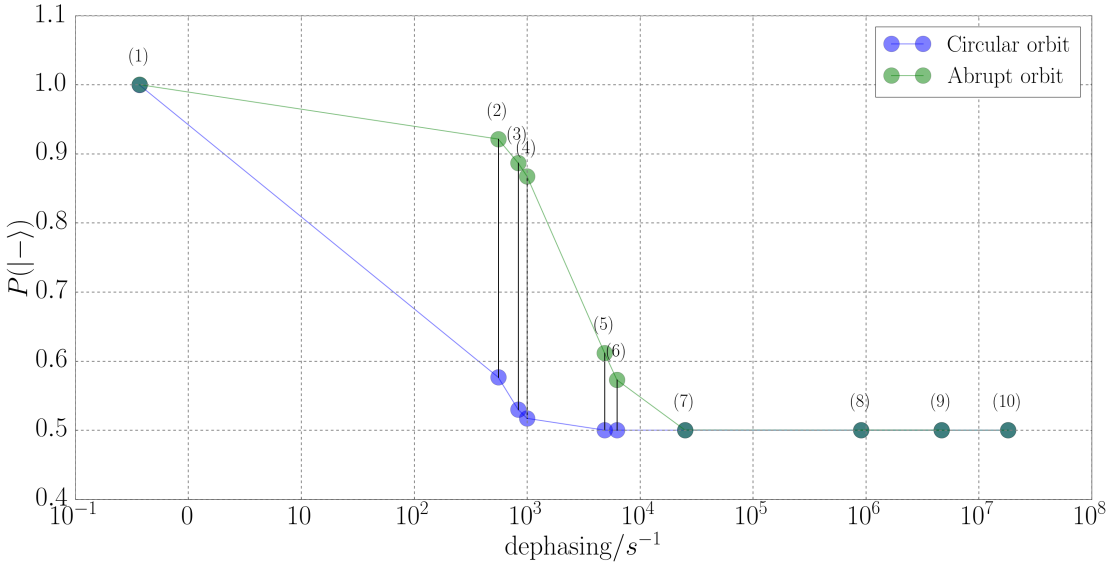

FIG. 4: A graph showing the relationship between the dephasing parameter Γ and the probability $P(|-\rangle)$ of measuring the probe qubit in the $|-\rangle$ state. In this simulation, one of the data qubits have undergone a bit-flip error. As the dephasing parameter increases, the probe qubit moves towards the maximally mixed state and the probability of measuring $|-\rangle$ goes towards 0.5.

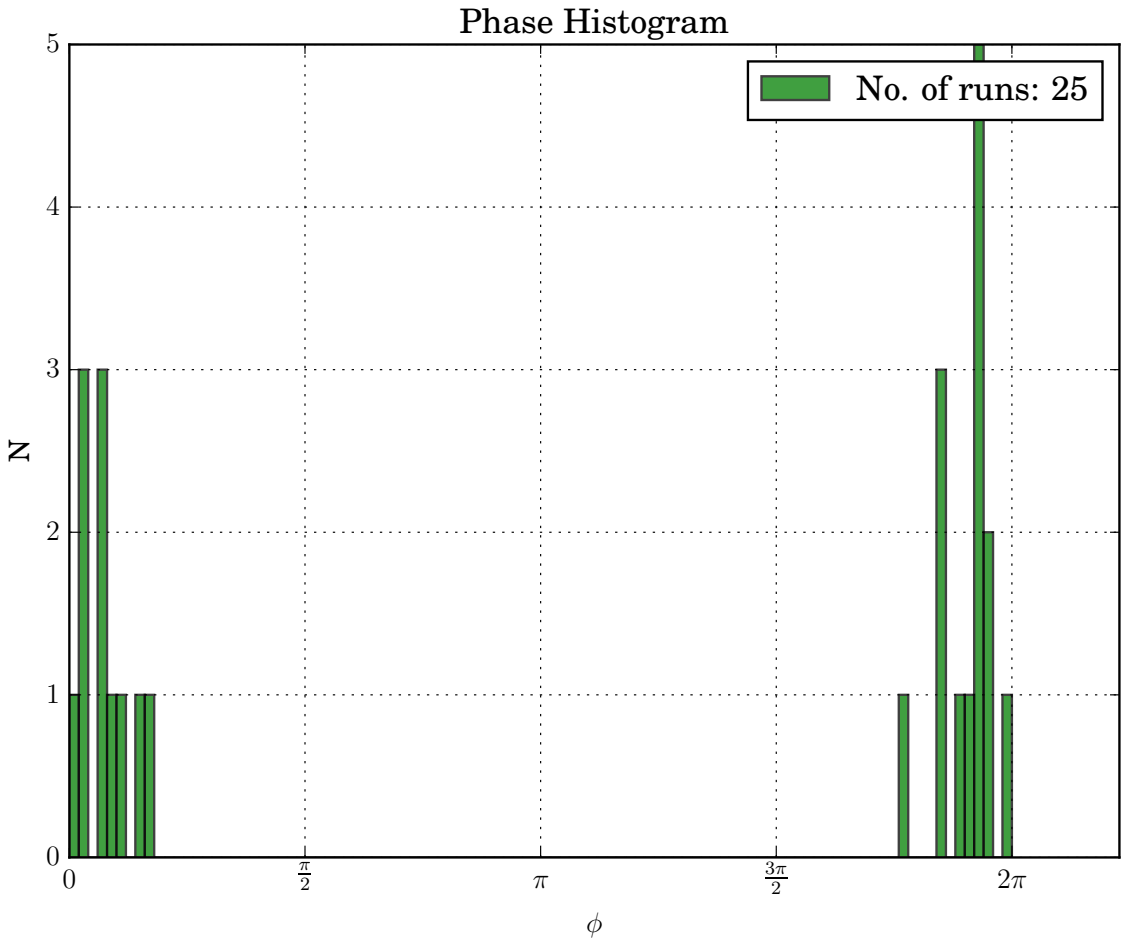

FIG. 5: Phase errors over 25 runs as a result of randomly generated data qubit displacements within a pillbox of half-height 3 nm and radius 6 nm. These values are a threshold for the proposed scheme.

FIG. 6: Phase errors as a result of misplaced data qubits.

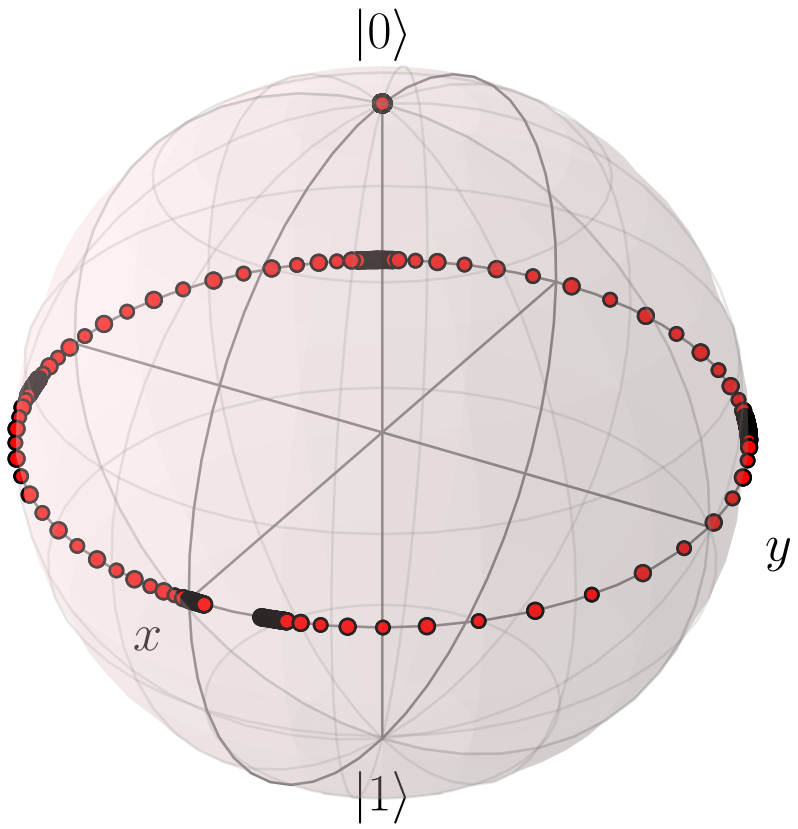

(a) Evolution of probe qubit with data qubit displacement in the Z direction. 1st and 2nd qubits are displaced 4 nm down, slowing the evolution, the 4th is displaced 3 nm up with a resultant increase in phase accumulated. The overall deviation from 2π is small as a result.